

# Bifurcations of planar balanced configurations for the $n$ -body problem in $\mathbb{R}^4$

Katharina Kormann and Giorgia Testolina

*Ruhr-Universität Bochum, Fakultät für Mathematik*

October 21, 2025

## Abstract

Central configurations play a fundamental role in the Newtonian  $n$ -body problem, as they give rise to motions in which the configuration evolves while preserving its shape up to rotation and scaling. These include relative equilibria, where the configuration rigidly rotates about the center of mass and each body moves along a circular orbit. For  $d \leq 3$ , such motions originate only from planar central configurations, whereas in higher dimensions the richer structure of the orthogonal group admits new balanced configurations that can produce non-planar relative equilibria. Building on the framework introduced in [4], we analyze bifurcations of planar balanced configurations in  $\mathbb{R}^4$ . We extend a classical variational result, which guarantees the existence of bifurcation points along trivial branches of critical points that are degenerate only at finitely many points, to the case where the trivial branch remains degenerate throughout. Applying this extension, we establish the existence of bifurcation points along the planar balanced configuration branch and derive a lower bound on their number.

**Acknowledgements** We would like to thank Luca Asselle for his support and help in revising this work and Alessandro Portaluri for the insightful discussions that contributed to the development of this work. The second author is partially funded by the CRC/TRR 191 “Symplectic structures in Geometry, Algebra and Dynamics” and by the DFG project 566804407 “Symplectic Dynamics, Celestial Mechanics and Magnetism”.

## 1 Introduction

The  $n$ -body problem is a cornerstone of celestial mechanics, which studies the motion of  $n$  point masses under their mutual gravitational attraction. Let  $m_1, \dots, m_n > 0$  be  $n$  point masses with positions  $q_1, \dots, q_n \in \mathbb{R}^d$ ,  $d \geq 2$ . Introducing the configuration vector  $q := (q_1, \dots, q_n) \in \mathbb{R}^{nd}$ , the diagonal mass matrix  $M := \text{diag}(m_1 \mathbb{I}_d, \dots, m_n \mathbb{I}_d)$ , and the Newtonian gravitational potential function

$$U(q) := \sum_{i < j} \frac{m_i m_j}{|q_i - q_j|},$$

Newton’s equations of motion are given by

$$\ddot{q} = M^{-1} \nabla U(q). \quad (1)$$

System (1) is invariant under the symmetries of the Euclidean group, which, by Noether's theorem, correspond to conserved quantities. In particular, invariance under translations implies conservation of total linear momentum. As a consequence, the center of mass

$$\bar{q} = \frac{1}{\bar{m}} \sum_{i=1}^n m_i q_i, \quad \bar{m} = \sum_{i=1}^n m_i,$$

moves with constant velocity and can therefore be fixed at the origin without loss of generality. Under this condition, and excluding collisions, the collision-free configuration space is defined by

$$\mathcal{C} := \{q \in \mathbb{R}^{dn} \mid \bar{q} = 0, q_i \neq q_j \text{ for } i \neq j\}.$$

For  $n \geq 3$ , system (1) is extremely difficult to solve, and in fact a complete explicit solution is known only in the case  $n = 2$ . A classical approach — pioneered by Euler and Lagrange and further developed by Albouy, Chenciner, Conley, Moeckel, Montgomery, and Smale, among others — is therefore to look for special configurations of the masses that give rise to simple types of motion. Among these, *central* and *balanced configurations*, play a fundamental role [1, 3, 10, 11].

A central configuration is a special arrangement of the masses such that the acceleration vector of each body points towards the center of mass, with magnitude proportional to its distance from the center of mass. Mathematically, this condition can be expressed as

$$M^{-1} \nabla U(q) + \lambda q = 0, \quad (2)$$

for some positive constant  $\lambda$ . The study of central configurations dates back to Euler (1767) and Lagrange (1772), who classified all central configurations for the three-body problem. For any choice of masses, there are three classes of collinear central configurations, corresponding to different orderings of the masses along the line, and two planar configurations, one for each orientation, where the masses form the vertices of an equilateral triangle. For more information about central configurations, we refer to the lectures by Moeckel [10, 11].

Central configurations give rise, in dimensions  $d \leq 3$ , to particularly simple solutions of the  $n$ -body problem:

- Every central configuration yields a *homothetic solution*, in which the configuration maintains its shape while receding from or collapsing toward the center of mass. These homothetic motions also describe the qualitative behaviour near total collisions: orbits approaching or receding from a total collapse are asymptotic to such solutions.
- Planar central configurations lead to *homographic solutions*, where each body follows a Keplerian orbit while the shape of the configuration is preserved up to scaling and rotation.
- A special case of homographic motion is the *relative equilibrium*, in which the bodies move on circular orbits and the configuration rotates rigidly about the center of mass with constant angular velocity.

The situation changes fundamentally when  $d \geq 4$ , as the richer structure of the orthogonal group allows for new types of balanced configurations [1]. This structure permits, for instance, simultaneous rotations in two mutually orthogonal planes with distinct angular velocities, giving

rise to new ways of balancing gravitational and centrifugal forces. As a consequence, relative equilibria are no longer restricted to planar configurations, and the motion does not necessarily remain planar.

In this article we focus on balanced configurations in  $\mathbb{R}^4$ . For a detailed discussion of balanced configurations, we refer the reader to [3, 11]. Let  $s > 1$  and define the matrices

$$S := \text{diag}(s, s, 1, 1), \quad \hat{S} := \text{diag}(S, \dots, S).$$

A balanced configuration  $q \in \mathbb{R}^{4n}$  is said to be balanced if it satisfies

$$M^{-1} \nabla U(q) + \lambda \hat{S} q = 0, \quad (3)$$

for some  $\lambda > 0$ . This equation is invariant under the  $SO(2) \times SO(2)$  action given by independent rotations in the  $\mathbb{R}^2 \times \{0\}$  and  $\{0\} \times \mathbb{R}^2$  planes. It follows that balanced configurations are never isolated: they occur in  $S^1$  families if they lie in one of the two coordinate planes, and in  $S^1 \times S^1$  families otherwise.

A fundamental property of central and balanced configurations is their variational characterization as critical points of the Newtonian potential  $U$  under suitable normalization constraints. This variational viewpoint allows one to apply several techniques to study the  $n$ -body problem. Among these, an important approach is based on bifurcation theory, where varying a physical parameter — such as the masses or the angular velocity — allows one to detect new families of solutions and gain deeper insight into the structure of central and balanced configurations. In finite-dimensional variational problems, bifurcation points are typically detected through jumps in the Morse index along trivial branches of critical points that are non-degenerate except at finitely many parameter values. A convenient way to encode these jumps is through the *spectral flow*, an integer-valued invariant that counts the net number of eigenvalues of a continuous family of self-adjoint Fredholm operators crossing zero [5, 6]. In [4], this framework was used to study bifurcations of collinear central configurations in  $\mathbb{R}^4$ , that is, configurations in which all bodies lie on a line contained in the plane  $\{0\} \times \mathbb{R}^2$ . The authors showed that these configurations form a trivial branch for every  $s > 1$ , and that their Morse index jumps at specific values of  $s$ . The non-trivial branches bifurcating from this family correspond to balanced configurations. The main difficulty — degeneracy due to rotational symmetry — was resolved by reducing the problem to  $\{0\} \times \mathbb{R}^2 \times \{0\}$ , where such configurations become non-degenerate. In this work, we extend these results to planar central configurations in  $\{0\} \times \mathbb{R}^2$ . These configurations also form trivial branches of critical points, but the classical bifurcation theory cannot be applied directly, since planar configurations are never isolated critical points due to rotational symmetry and may in fact be Morse–Bott degenerate. This degeneracy prevents us from quotienting out the  $SO(2)$ -action induced by planar rotations. Our main contribution is therefore to develop a refined variational argument that applies to trivial branches of critical points which remain degenerate for all parameter values.

**Theorem 1.** *Let  $(F_s)_{s \in I}$  be a  $\mathcal{C}^2$  family of functionals on a finite-dimensional smooth manifold  $M$ , and let  $(q_s)_{s \in I}$  be a trivial branch of critical points of  $F_s$ . Denote by  $(H_s)_{s \in I}$  the corresponding Hessians at  $q_s$ . Suppose that there exist  $k$  smooth functions  $s \mapsto v_i(s)$  such that the vectors  $\{v_1(s), \dots, v_k(s)\}$  are linearly independent for every  $s \in I$  and:*

- *for all  $s \in I$ ,  $\text{Span}\{v_1(s), \dots, v_k(s)\} \subseteq \ker H_s$ ,*
- *for all  $s \in I \setminus J$ ,  $\ker H_s = \text{Span}\{v_1(s), \dots, v_k(s)\}$ ,*

where  $J \subset I$  is a finite set. Then the spectral flow  $\text{sf}(H_s, s \in I)$  is well-defined on  $I$ . Moreover, if it is nonzero, then there exists at least one bifurcation instant from the trivial branch.

As a direct application of the theorem above, we obtain the following result for the family of planar balanced configurations:

**Theorem 2.** *Let  $s_1, s_2 > 1$ , and let  $(\hat{q}_s)_{s \in [s_1, s_2]}$  denote the trivial branch of solutions generated by a planar central configuration in the plane  $\{0\} \times \mathbb{R}^2$ . For  $s_1$  sufficiently close to 1 and  $s_2$  sufficiently large, there exists at least one bifurcation point along the trivial branch.*

We conclude by presenting numerical simulations of non-trivial branches bifurcating from the trivial branches of planar central configurations for  $n = 4$  and  $n = 5$ . For instance, we find that the planar central configuration with four equal masses placed at the vertices of a square is connected to the regular tetrahedron at  $s = 1$  through a family of balanced configurations. A similar behaviour is observed for a planar central configuration with three equal masses at the vertices of an equilateral triangle and a mass at the center of mass. The nature of the these configurations changes depending on the mass value at the center. In particular, there exists a critical mass value  $m^*$ , which corresponds to the point where the planar central configuration becomes Morse-Bott degenerate; this marks the threshold where the nature of the configurations changes.

## 2 Balanced configurations: definition and main properties

In this section, we recall the definition of balanced configurations in  $\mathbb{R}^4$  and summarize their main properties. For further details see [3, 11].

Consider  $n$  point masses  $m_1, \dots, m_n > 0$  with positions  $q_1, \dots, q_n \in \mathbb{R}^4$  moving according to Newton's law of gravitation

$$\ddot{q} = M^{-1} \nabla U(q) \quad (4)$$

where  $q := (q_1, \dots, q_n) \in \mathbb{R}^{4n}$  and  $M := \text{diag}(m_1 \mathbb{I}_4, \dots, m_n \mathbb{I}_4)$ . As before, we restrict our attention to the collision-free configuration space with center of mass at the origin

$$\mathcal{C} = \{q \in \mathbb{R}^{4n} \mid \bar{q} = 0, q_i \neq q_j \text{ for } i \neq j\}.$$

Let  $s > 1$  be a positive real number, and define the matrices

$$S := \text{diag}(s, s, 1, 1) \in \mathbb{R}^{4 \times 4}, \quad \hat{S} := \text{diag}(S, \dots, S) \in \mathbb{R}^{4n \times 4n}.$$

**Definition 2.1.** A balanced configuration is an arrangement of the masses that satisfies the equation

$$M^{-1} \nabla U(q) + \lambda \hat{S} q = 0, \quad (5)$$

where  $\lambda > 0$  is a positive constant.

**Remark 2.2.** As pointed out by Asselle and Portaluri [3], this definition is equivalent to that of Albouy and Chenciner [1], also used by Moeckel [11], where  $S$  is a symmetric positive definite matrix. Since the problem is invariant under orthogonal changes of coordinates, one may always assume that  $S$  is diagonal, i.e. that the spectral basis of  $S$  coincides with the canonical basis of

$\mathbb{R}^4$ . It is also often required that  $S = -A^2$  with  $A$  skew-symmetric matrix. In particular, in even dimension this condition ensures that every balanced configuration generates a relative equilibrium of the  $n$ -body problem.

Balanced configurations strictly contain central configurations. Indeed, by setting  $s = 1$  in equation (5), we recover the central configuration equation

$$M^{-1}\nabla U(q) + \lambda q = 0. \quad (6)$$

The main difference is that any balanced configuration can produce a relative equilibrium solution of (4) of the form

$$q(t) := \begin{pmatrix} e^{i\sqrt{s\lambda}t} & 0 \\ 0 & e^{i\sqrt{\lambda}t} \end{pmatrix} \cdot q$$

whereas only planar central configurations give rise to relative equilibria. Furthermore, in the balanced case, the motion does not necessarily have to be periodic, but it can be quasi-periodic when  $\sqrt{s}$  is irrational. This difference follows from the fact that central configurations are invariant under the  $SO(4)$ -group, while balanced configurations are invariant under the  $SO(2) \times SO(2)$  action given by rotations in the  $\mathbb{R}^2 \times \{0\}$  and  $\{0\} \times \mathbb{R}^2$  planes. In particular, balanced configurations are never isolated but come in  $S^1$  families if they belong to one of the two planes mentioned above and in  $S^1 \times S^1$  families otherwise.

We define the weighted scalar product  $\langle \cdot, \cdot \rangle_S$  as

$$\langle \cdot, \cdot \rangle_S := \langle \hat{S}M \cdot, \cdot \rangle.$$

Observing that the Newtonian potential  $U(q)$  is homogeneous of degree  $-1$ , and applying Euler's theorem for homogeneous functions, we are able to determine the value of the constant  $\lambda$  in equation (5):

$$\lambda = \frac{U(q)}{|q|_S^2}.$$

It follows immediately from Definition 2.1 that if  $q$  is a balanced configuration, then  $kq$  is also a balanced configuration for any  $k \in \mathbb{R}$ . Therefore, we can restrict our attention to the collision free configuration sphere

$$\mathcal{S} := \{q \in \mathcal{C} \mid |q|_S^2 = 1\}.$$

The manifold  $\mathcal{S}$  is an open subset of a smooth compact manifold diffeomorphic to a  $(4n - 5)$ -dimensional sphere. Moreover, since in  $\mathcal{S}$  we have  $\lambda = U(q)$ , equation (5) becomes

$$M^{-1}\nabla U(q) + U(q)\hat{S}q = 0. \quad (7)$$

Finally, we describe the variational characterization of balanced configurations, a key feature that will play a fundamental role in our discussion. The proof of this theorem can be found in [11].

**Theorem 2.3.** *A configuration  $q$  is a balanced configuration if and only if it is a critical point of  $U|_{\mathcal{S}}$ .*

Thus, the problem of finding balanced configuration is essentially that of finding critical points of  $U|_{\mathcal{S}}$  or, equivalently, rest points of the gradient flow of  $U|_{\mathcal{S}}$ . The Hessian of  $U|_{\mathcal{S}} : \mathcal{S} \rightarrow \mathbb{R}$  at a critical point  $q$  is the quadratic form on  $T_q \mathcal{S}$  represented, with respect to the mass scalar product  $\langle M \cdot, \cdot \rangle$ , by the  $(4n \times 4n)$ -matrix

$$H(q) = M^{-1} D^2 U(q) + \hat{S} U(q).$$

A straightforward computation shows that the  $(i, j)$ -th entry of  $D^2 U(q)$  is given by

$$\begin{aligned} D_{ij} &= \frac{m_i m_j}{r_{ij}^3} (\mathbb{I}_4 - 3u_{ij} u_{ij}^t) \quad \text{for } i \neq j \\ D_{ii} &= - \sum_{j \neq i} D_{ij} \end{aligned}$$

where  $r_{ij} := |q_i - q_j|$  and  $u_{ij} := \frac{q_i - q_j}{|q_i - q_j|}$ . The rotational invariance described above implies that balanced configurations are never isolated critical points of  $U|_{\mathcal{S}}$  and that the Hessian is always degenerate. We say that a balanced configuration is Morse-Bott non-degenerate if its nullity is as small as possible, given the rotational symmetry.

### 3 Morse index of planar balanced configurations

The aim of this section is to analyze how the inertia indices of planar balanced configurations lying in the plane  $\{0\} \times \mathbb{R}^2$  depend on the parameter  $s$ .

To reduce the effect of rotational symmetry, we restrict our attention to spatial configurations contained in  $\{0\} \times \mathbb{R}^3 \subset \mathbb{R}^4$ . The associated configuration space is

$$\hat{\mathcal{S}} = \{q \in \mathcal{S} \mid q_i \in \{0\} \times \mathbb{R}^3 \forall i = 1, \dots, n\} \subset \mathcal{S}.$$

Identifying  $\{0\} \times \mathbb{R}^3$  with  $\mathbb{R}^3$ , the matrix  $S$  in the balanced configuration equation reduces to

$$S = \text{diag}(s, 1, 1).$$

Hence, balanced configurations occur in  $S^1$ -families, corresponding to the  $SO(2)$ -action generated by rotations in the plane  $\{0\} \times \mathbb{R}^2$  (rather than the  $S^1 \times S^1$ -families that may arise in  $\mathbb{R}^4$ ). Moreover, by the  $45^\circ$ -Theorem for balanced configurations, the action is free on  $\hat{\mathcal{S}} \setminus \mathcal{C}_{\text{coll}}$ , where  $\mathcal{C}_{\text{coll}}$  denotes the manifold of collinear configurations. Thus, working in  $\mathbb{R}^3$  with  $\hat{S} = \text{diag}(s, 1, 1)$  yields a simpler yet equivalent setting for analyzing planar bifurcations.

**Remark 3.1.** The classical  $45^\circ$ -Theorem for collinear central configurations states that the manifold of collinear configurations is an attractor for the projectivized gradient flow of  $U|_{\mathcal{S}}$ : trajectories starting near it become increasingly collinear, and no non-collinear central configurations exist in its neighborhood. For balanced configurations, this property holds only for configurations collinear along the  $e_1$ -axis, which corresponds to the eigenvector associated with the distinct eigenvalue  $s > 1$  of  $S = \text{diag}(s, 1, 1)$ . For certain values of  $s$ , however, collinear balanced configurations along other lines may become local minima of  $U|_{\mathcal{S}}$ , and therefore do not satisfy the  $45^\circ$ -Theorem; for more details see [3] and reference therein. In  $\mathbb{R}^4$ , the manifold  $\mathcal{C}_{\text{coll}}$  of configurations collinear along

the  $e_1$ -axis coincides with the singular set of the  $SO(2)$ -action generated by rotations in the plane  $\{0\} \times \mathbb{R}^2$ . Hence, this collinear set can be safely removed before performing the  $SO(2)$ -reduction, yielding a smooth quotient

$$\bar{\mathcal{S}} = (\mathcal{S} \setminus \mathcal{C}_{\text{coll}})/SO(2).$$

With these preliminaries in place, we proceed to analyze planar balanced configurations in the plane  $\{0\} \times \mathbb{R}^2$ . Let  $\hat{q}$  denote one such configuration. We observe that this is, in fact, a central configuration for all  $s > 1$ . By rearranging the coordinates of  $\hat{q}$  as  $(x_1, \dots, x_n, y_1, \dots, y_n, z_1, \dots, z_n)$ , the Hessian matrix can be decomposed into the following block form:

$$H(\hat{q}) = \begin{pmatrix} M^{-1}B(\hat{q}) & 0 \\ 0 & M^{-1}D(\hat{q}) \end{pmatrix} + \begin{pmatrix} sU(\hat{q})I_n & 0 \\ 0 & U(\hat{q})I_{2n} \end{pmatrix}$$

Here:

- $B(\hat{q})$  is an  $n \times n$  matrix, where the  $(i, j)$ -th entry is given by

$$b_{ij} = \frac{m_i m_j}{r_{ij}^3}, \quad b_{ii} = - \sum_{j \neq i} b_{ij};$$

- $D(\hat{q})$  is a  $2n \times 2n$  block matrix, with its blocks defined as

$$D_{ij} = \frac{m_i m_j}{r_{ij}^3} \begin{pmatrix} 1 - 3 \cos^2 \theta_{ij} & -3 \sin \theta_{ij} \cos \theta_{ij} \\ -3 \sin \theta_{ij} \cos \theta_{ij} & 1 - 3 \sin^2 \theta_{ij} \end{pmatrix}, \quad D_{ii} = - \sum_{j \neq i} D_{ij},$$

where  $\theta_{ij}$  is the angle between the vector  $(q_i - q_j)$  and the  $y$ -axis in  $\mathbb{R}^3$ .

Using this decomposition, we define:

- the normal inertia indices,  $(\iota_n^-(\hat{q}), \iota_n^0(\hat{q}), \iota_n^+(\hat{q}))$ , which correspond to the inertia indices of  $M^{-1}B(\hat{q}) + sU(\hat{q})\mathbb{I}_n$ ;
- the planar inertia indices,  $(\iota_p^-(\hat{q}), \iota_p^0(\hat{q}), \iota_p^+(\hat{q}))$ , which correspond to the inertia indices of  $M^{-1}D(\hat{q}) + U(\hat{q})\mathbb{I}_{2n}$ .

**Remark 3.2.** For a planar central configuration, it is known that  $\iota_n^0(\hat{q}) \geq 2$  and  $\iota_p^0(\hat{q}) \geq 1$ , with equality holding only if  $\hat{q}$  is Morse-Bott non-degenerate, i.e. its nullity is minimal given the rotational symmetry.

From the formula for the Hessian matrix, it is evident that the planar inertia indices remain unchanged as  $s$  varies. In particular, the planar nullity is always at least 1, implying that a planar balanced configuration  $\hat{q}$  is degenerate as a critical point of  $U|_{\mathcal{S}}$  for every choice of  $s > 1$ . We now provide a complete characterization of the normal inertia indices, depending on the spectrum of the matrix  $M^{-1}B(\hat{q})$  and the parameter  $s$ . The  $(n \times n)$ -matrix  $M^{-1}B(\hat{q})$  has one null eigenvalue which does not contribute to the inertia indices, since its corresponding eigenvector  $(1, \dots, 1)$  is transverse to the tangent space  $T_{\hat{q}}\hat{\mathcal{S}}$ . Of the other  $(n - 1)$  eigenvalues, at least 2 are equal to  $-U(\hat{q})$ . Moreover, if we have more than three masses, there always exists at least one eigenvalue smaller than  $-U(\hat{q})$ . The existence of these eigenvalues will play a crucial role in the following analysis,

since they will be relate to the values of  $s$  at which bifurcations occur. We denote the distinct eigenvalues of  $M^{-1}B(\hat{q})$  by

$$\mu_k(\hat{q}) < \cdots < \mu_l(\hat{q}) = -U(\hat{q}) < \cdots < 0 < \cdots < \mu_1$$

and their corresponding multiplicity by  $\alpha_1, \dots, \alpha_k$  with  $\alpha_l \geq 2$  and  $k > l$ .

**Proposition 3.3.** *Let  $\hat{q}$  be a planar balanced configuration in the plane  $\{0\} \times \mathbb{R}^2$ . The normal inertia indices of  $\hat{q}$  vary with the parameter  $s$  as follows:*

(i) *If  $-\frac{\mu_i}{U(\hat{q})} < s < -\frac{\mu_{i+1}}{U(\hat{q})}$  for some  $i \in \{l, \dots, k-1\}$ , then*

$$\iota_n^0(\hat{q}) = 0, \quad \iota_n^+(\hat{q}) = \sum_{j=1}^i \alpha_j, \quad \iota_n^-(\hat{q}) = n-1 - \sum_{j=1}^i \alpha_j.$$

(ii) *If  $s = -\frac{\mu_i}{U(\hat{q})}$  for some  $i \in \{l+1, \dots, k\}$ , the  $i$ -th eigenvalue vanishes and contributes its multiplicity  $\alpha_i$  to the nullity:*

$$\iota_n^0(\hat{q}) = \alpha_i, \quad \iota_n^+(\hat{q}) = \sum_{j=1}^{i-1} \alpha_j, \quad \iota_n^-(\hat{q}) = n-1 - \sum_{j=1}^i \alpha_j.$$

(iii) *For  $s > -\frac{\mu_k}{U(\hat{q})}$ , all eigenvalues are positive and*

$$\iota_n^0(\hat{q}) = 0, \quad \iota_n^+(\hat{q}) = n-1, \quad \iota_n^-(\hat{q}) = 0.$$

*Proof.* The operator  $M^{-1}B(\hat{q}) + sU(\hat{q})I_n$  has eigenvalues

$$\mu_j + sU(\hat{q}), \quad j = 1, \dots, k,$$

each with multiplicity  $\alpha_j$ . Hence the inertia indices are determined entirely by the signs of these shifted eigenvalues. In particular, for any  $s > 1$ , all eigenvalues  $\mu_j \geq -U(\hat{q})$  always contribute to the Morse coindex, while a change in the inertia occurs precisely when some  $\mu_j + sU(\hat{q})$  crosses zero.

If  $-\mu_i/U(\hat{q}) < s < -\mu_{i+1}/U(\hat{q})$ , then  $\mu_{i+1} + sU(\hat{q}) < 0 < \mu_i + sU(\hat{q})$  and the first  $i+1$  eigenvalues become positive by adding  $sU(\hat{q})$ . At  $s = -\mu_i/U(\hat{q})$ , the  $i$ -th eigenvalue vanishes, so its multiplicity  $\alpha_i$  contributes to the nullity. Finally, when  $s > -\mu_k/U(\hat{q})$ , all shifted eigenvalues are strictly positive, so the coindex equals  $n-1$  and both index and nullity vanish.  $\square$

This proposition shows that the Morse index  $\iota^- = \iota_n^- + \iota_p^-$  of  $\hat{q}$  jumps at precise values of  $s$  that depend on the spectrum of  $M^{-1}B(\hat{q})$  and the value of  $U(\hat{q})$ . Moreover, the normal nullity  $\iota_n^0$  is equal to zero, except for finitely many values of  $s$ .

## 4 Spectral flow and bifurcation results in finite dimension

The notion of spectral flow was introduced by Atiyah, Patodi and Singer [5] in the study of elliptic operators on manifolds. It is a homotopy invariant of continuous paths of self-adjoint Fredholm

operators on a real Hilbert space, and it counts the net number of eigenvalues crossing zero along the path. This quantity plays a central role in index theory, Morse theory on Hilbert manifolds, and bifurcation problems in infinite dimension (see, e.g., [6, 7, 8, 12]). In this chapter we restrict to the finite-dimensional setting, and use the spectral flow of a family of Hessians to detect bifurcation points along trivial branches of critical points.

Let  $(E, \langle \cdot, \cdot \rangle)$  be an Euclidean space and  $\mathcal{L}_{\text{sym}}(E)$  be the vector space of all linear self-adjoint operators in  $E$ .

**Definition 4.1.** The *spectral flow* of a continuous path  $L : [a, b] \rightarrow \mathcal{L}_{\text{sym}}(E)$  of self-adjoint operators with invertible endpoints is the integer

$$\text{sf}(L_t, t \in [a, b]) := \iota^-(L_a) - \iota^-(L_b), \quad (8)$$

where  $\iota^-$  denotes the number of negative eigenvalues of the operator  $L_t$ . A path  $L$  with invertible endpoints is said to be admissible.

In other words, the spectral flow represents the net change in the number of negative eigenvalues of  $L(t)$  as  $t$  runs from  $a$  to  $b$ , as it quantifies the difference between the eigenvalues crossing 0 from left to right and the eigenvalues crossing 0 from right to left.

Given a continuous family of  $\mathcal{C}^2$  functionals admitting a trivial branch of critical points, we consider the corresponding family of Hessians evaluated along this branch. The non-vanishing of the spectral flow of these Hessians ensures the existence of bifurcations of nontrivial critical points. Additionally, it provides an estimate on the number of bifurcation points along the branch. In this context, we recall the geometric framework used in [4, Section 3], that allows to extend this result to a one-parameter  $\mathcal{C}^2$ -family of functions defined on a finite-dimensional manifold.

Let  $M$  be a finite-dimensional Riemannian manifold and let  $\pi : M \rightarrow I$ , with  $I = [a, b]$ , be a smooth submersion. For each  $\lambda \in I$ , the fiber

$$M_\lambda := \pi^{-1}(\lambda)$$

is a smooth codimension-one submanifold of  $M$ , and its tangent space at  $x \in M_\lambda$  is given by

$$T_x M_\lambda = \ker D\pi_x.$$

Collecting these tangent spaces defines the vertical tangent bundle

$$T^v M = \{\ker D\pi_x \mid x \in M\} \subset TM.$$

Let  $F : M \rightarrow \mathbb{R}$  be a smooth function. For  $\lambda \in I$ , the restriction of  $F$  to each fiber  $M_\lambda$  gives a family of smooth functions  $F_\lambda : M_\lambda \rightarrow \mathbb{R}$ . A smooth section  $\gamma : I \rightarrow M$  is called a *trivial branch of critical points* if  $\gamma(\lambda)$  is a critical point of  $F_\lambda$  for every  $\lambda \in I$ .

**Definition 4.2.** A point  $\lambda_* \in I$  is a *bifurcation instant* from the trivial branch  $\gamma(I)$  if there exists a sequence  $\lambda_n \rightarrow \lambda_*$  and a sequence of critical points  $x_n \in M_{\lambda_n}$  for  $F_{\lambda_n}$  converging to  $\gamma(\lambda_*)$  such that  $\pi(x_n) = \lambda_n$  and  $x_n \notin \gamma(I)$ .

For each  $\lambda \in I$ , let  $H_\lambda$  denote the Hessian of  $F_\lambda$  at  $\gamma(\lambda)$ . The family  $(H_\lambda)_{\lambda \in I}$  defines a smooth function  $h$  on the total space of the pullback bundle

$$\mathcal{H} = \gamma^*(T^v M),$$

By restricting  $h$  to the fibers  $T_{\gamma(\lambda)}M_\lambda$  of  $\mathcal{H}$ , we obtain a family of (generalized) quadratic forms  $H_\lambda$  defined on  $T_{\gamma(\lambda)}M_\lambda$ .

We are now ready to state the following abstract bifurcation theorem, for the proof see [4, Theorem 4.4].

**Theorem 4.3.** *Let  $(H_\lambda)_{\lambda \in I}$ , with  $I = [a, b]$  be an admissible path of Hessians such that the spectral flow*

$$\text{sf}(H_\lambda, \lambda \in I) \neq 0.$$

*Then there exists at least one bifurcation instant  $\lambda_* \in (a, b)$  of critical points of  $F$  from the trivial branch  $\gamma(I)$ . Moreover, if  $\ker H_\lambda \neq \{0\}$  only for finitely many  $\lambda$ , then there are at least*

$$\left\lfloor \frac{\text{sf}(H_\lambda, \lambda \in I)}{m} \right\rfloor$$

*distinct bifurcation instants in  $(a, b)$ , where  $m := \max\{\dim \ker H_\lambda\}$ .*

The next theorem generalizes this result to the case where the family of Hessians  $(H_\lambda)_{\lambda \in I}$  is singular for every  $\lambda \in I$  and the kernel of  $H_\lambda$  “varies smoothly” with respect to  $\lambda$ , as specified in the following theorem. This is the key tool for treating planar configurations which are Morse-Bott degenerate.

**Theorem 4.4.** *Suppose that there exist  $k$  smooth functions  $\lambda \mapsto v_i(\lambda)$ ,  $i = 1, \dots, k$ , such that the vectors  $\{v_1(\lambda), \dots, v_k(\lambda)\}$  are linearly independent for every  $\lambda \in I$  and:*

- for all  $\lambda \in I$ ,  $\text{Span}\{v_1(\lambda), \dots, v_k(\lambda)\} \subseteq \ker H_\lambda$ ,
- for all  $\lambda \in I \setminus J$ ,  $\ker H_\lambda = \text{Span}\{v_1(\lambda), \dots, v_k(\lambda)\}$ ,

where  $J \subset I$  is finite. Denote by  $K_\lambda = \text{Span}\{v_1(\lambda), \dots, v_k(\lambda)\}$ . Let  $W_\lambda = T_{\gamma(\lambda)}M_\lambda/K_\lambda$  and let  $\bar{H}_\lambda = H_\lambda|_{W_\lambda}$  be the restriction of the Hessian at  $\gamma(\lambda)$  to the quotient space. Then the path  $(\bar{H}_\lambda)_{\lambda \in I}$  is degenerate only at finitely many values of  $\lambda$ . Moreover, if it is admissible and the spectral flow  $\text{sf}(\bar{H}_\lambda, \lambda \in I)$  is nonzero, then the conclusions of Theorem 4.3 hold.

*Proof.* Let  $\{v_1(\lambda), \dots, v_k(\lambda)\}$  be a smooth family of vectors spanning the subspace  $K_\lambda$ , where

- for  $\lambda \in I$ ,  $K_\lambda \subseteq \ker H_\lambda$ ,
- for  $\lambda \in I \setminus J$ ,  $K_\lambda = \ker H_\lambda$ .

For each  $\lambda \in I$ , extend  $\{v_1(\lambda), \dots, v_k(\lambda)\}$  to an orthonormal basis

$$\{v_1(\lambda), \dots, v_k(\lambda), w_{k+1}(\lambda), \dots, w_n(\lambda)\}$$

of  $T_{\gamma(\lambda)}M_\lambda$  with respect to the Riemannian metric on  $M$ .

Let  $L_\lambda$  be the self-adjoint operator associated with the quadratic form  $H_\lambda$ , so that for all  $u \in T_{\gamma(\lambda)}M_\lambda$ ,

$$H_\lambda(u) = \langle L_\lambda u, u \rangle.$$

In the orthonormal basis above,  $L_\lambda$  takes the block-diagonal form

$$L_\lambda = \begin{pmatrix} \mathbb{O}_k & 0 \\ 0 & \bar{L}_\lambda \end{pmatrix},$$

where

- $\mathbb{O}_k$  is the  $k \times k$  zero matrix corresponding to  $K_\lambda$ , since  $K_\lambda \subseteq \ker H_\lambda$ ,
- $\bar{L}_\lambda$  is a self-adjoint operator acting on the quotient space  $W_\lambda = T_{\gamma(\lambda)} M_\lambda / K_\lambda$ , representing the restriction of  $H_\lambda$  to  $W_\lambda$ .

Thus, the bifurcation problem reduces to studying the family of quadratic forms

$$\bar{H}_\lambda := H_\lambda|_{W_\lambda}.$$

The smooth dependence of  $\lambda \mapsto \bar{L}_\lambda$  implies that  $\bar{H}_\lambda$  is degenerate only at isolated points, i.e. for finitely many  $\lambda \in J$ . If the path  $(\bar{H}_\lambda)_{\lambda \in I}$  is admissible and the spectral flow  $\text{sf}(\bar{H}_\lambda, \lambda \in I)$  is nonzero, then the conclusions of Theorem 4.3 apply.  $\square$

**Remark 4.5.** A particular case of this theorem is when the subspace  $K_\lambda$  remains constant for all  $\lambda \in I$ . In the next section, we will use this specific case to establish the existence of bifurcations for planar balanced configurations.

## 5 Bifurcations of planar balanced configurations

We now combine the inertia index analysis of Section 3 with the spectral flow framework of Section 4 to establish bifurcations along trivial branches of planar balanced configurations in  $\{0\} \times \mathbb{R}^2$ . Recall that such configurations are central configurations and solve the balanced configuration equation (5) for all  $s > 1$ .

**Theorem 5.1.** *Let  $s_1, s_2 > 1$  and set  $I := [s_1, s_2]$ . Fix a planar balanced configuration  $\hat{q}$  lying in the  $\{0\} \times \mathbb{R}^2$ -plane, and consider the associated trivial family  $(\hat{q}_s)_{s \in I}$  defined by  $\hat{q}_s = \hat{q}$  for all  $s \in I$ . If  $s_1$  is chosen sufficiently close to 1 and  $s_2$  is taken large enough, then, with*

$$\alpha := \sum_{j=1}^l \alpha_j, \quad \beta := \max\{\alpha_i \mid i = l+1, \dots, k\},$$

there exist at least

$$\left\lfloor \frac{n-1-\alpha}{\beta} \right\rfloor$$

distinct bifurcation instants branching from  $\hat{q}$ .

*Proof.* Let  $\hat{\mathcal{S}}_s$  denote the balanced configuration space corresponding to the parameter  $s$ . Define the total space

$$\mathcal{E} := I \times \hat{\mathcal{S}}_s,$$

which is the trivial bundle over  $I$  with fiber  $\hat{\mathcal{S}}_s$ . We denote by  $\pi : \mathcal{E} \rightarrow I$  the canonical projection, so that  $\pi^{-1}(s) = \hat{\mathcal{S}}_s$ . Restricting the Newtonian potential  $U$  to  $\mathcal{E}$  yields a smooth bundle map  $\mathcal{U} : \mathcal{E} \rightarrow \mathbb{R}$ , whose fiberwise restriction is  $\mathcal{U}_s = U|_{\hat{\mathcal{S}}_s}$ .

Let  $H_s$  be the quadratic form given by the Hessian of  $U$  at  $\hat{q}_s$ . Because of rotational symmetry,  $H_s$  is degenerate for every  $s \in I$ . From the results of Section 3, the kernel of  $H_s$  is constant for all but finitely many values of  $s$ , and it coincides with the kernel of the planar Hessian

$$M^{-1} D^2 U(\hat{q}) + s U(\hat{q}) I_{2n}.$$

Denote this kernel by  $K$ . Thus,

- for  $s \in I$ , one has  $K \subseteq \ker H_s$ ,
- for  $s \in I \setminus J$ , one has  $\ker H_s = K$ ,

where  $J \subset I$  is a finite set consisting of the parameter values

$$-\frac{\mu_i}{U(\hat{q})}, \quad i = l+1, \dots, k.$$

Passing to the quotient space  $T_{\hat{q}_s} \hat{\mathcal{S}}_s / K$ , we obtain the restricted Hessians  $\bar{H}_s$ . By construction,  $\bar{H}_s$  is non-degenerate except when  $s \in J$ . Now choose  $s_1, s_2 \in I$  satisfying

$$1 < s_1 < -\frac{\mu_{l+1}}{U(\hat{q})}, \quad s_2 > -\frac{\mu_k}{U(\hat{q})}.$$

For this choice, the path  $s \mapsto \bar{H}_s$  is admissible. Applying part (i) of Proposition 3.3 with  $i = l$  gives

$$\iota_n^-(\hat{q}_{s_1}) = n - 1 - \alpha,$$

while part (iii) yields

$$\iota_n^-(\hat{q}_{s_2}) = 0.$$

Hence the spectral flow along  $s \in I$  is

$$\text{sf}(H_s, s \in I) = \iota_n^-(H_{s_1}) - \iota_n^-(H_{s_2}) = n - 1 - \alpha.$$

Since the kernel of  $\bar{H}_s$  is non-trivial only at eigenvalues  $\mu_i$  for  $i \in \{l+1, \dots, k\}$ , each with multiplicity  $\alpha_i$ , Theorem 4.4 applies.  $\square$

**Remark 5.2.** Theorem 5.1 applies whether the planar balanced configuration  $\hat{q}$  is degenerate or Morse-Bott non-degenerate. In the case of Morse-Bott non-degenerate planar balanced configurations, where the planar nullity is always 1, it is sufficient to consider the quotient space  $\bar{\mathcal{S}} = (\hat{\mathcal{S}} \setminus \mathcal{C}_{\text{coll}})/SO(2)$ , where  $\mathcal{C}_{\text{coll}}$  denotes the manifold of collinear configurations contained in  $\mathbb{R} \times \{0\}$ . In this case, planar balanced configuration restricted to the quotient manifold become non-degenerate critical point and it is sufficient to apply Theorem 4.3.

## 6 Numerical simulations for planar balanced configurations

In this section, we present numerical examples of non-trivial branches of balanced configurations that bifurcate from planar central configurations. The simulations were obtained using a continuation method based on a program originally developed by Fenucci in [4] for collinear central configurations in the three-body problem and adapted here to the planar setting.

The continuation method [2] is a numerical technique for tracing families of solutions of parametric nonlinear systems of the form

$$F(q, s) = 0,$$

where  $q \in \mathbb{R}^d$  and  $s \in \mathbb{R}$ . Starting from a known solution  $(q_i, s_i)$ , the goal is to compute new solutions for different values of the parameter  $s$ . At each step, we displace  $(q, s)$  by a step  $\delta$  and solve the system

$$\begin{cases} F(q, s) = 0, \\ |(q, s) - (q_i, s_i)|^2 - \delta^2 = 0, \end{cases}$$

using a damped Newton's method, whose Jacobian has the form

$$\begin{pmatrix} \frac{\partial F}{\partial q} & \frac{\partial F}{\partial s} \\ 2(q - q_i) & 2(s - s_i) \end{pmatrix}.$$

An initial guess is obtained by starting from the known solution  $(q_i, s_i)$  and taking a tangent displacement along the curve of solutions.

In our case, the system is given by the balanced configuration equation

$$F(q, s) = M^{-1} \nabla U(q) + U(q) \hat{S}(s) q.$$

Starting from a planar central configuration  $\hat{q}$ , which produces a trivial branch of solutions, we compute the parameters  $\tilde{s}$  at which the configuration becomes degenerate, and hence bifurcations arise. We then displace  $\tilde{s}$  by setting  $s = \tilde{s} + \Delta s$  and compute a new solution using Newton's method. An initial guess is constructed by displacing  $\hat{q}$  along the direction of the kernel of  $\frac{\partial F}{\partial q}$ . These two solutions are then used to initialize the continuation method.

## 6.1 Examples for $n = 4$

We first consider four equal unit masses at the vertices of a square. The trivial branch of planar balanced configurations undergoes a bifurcation at  $\bar{s} = 1.4$ , from which a non-trivial branch emerges. Along this branch, the parameter  $s$  decreases, while the masses move to form the vertices of a tetrahedron. At  $s = 1$ , the configuration becomes a regular tetrahedron, corresponding to a spatial central configuration for the four-body problem (see Figure 1). All configurations along this branch are local minima of the potential function  $U|_{\mathcal{S}}$ , whereas the initial planar configuration is a saddle point.

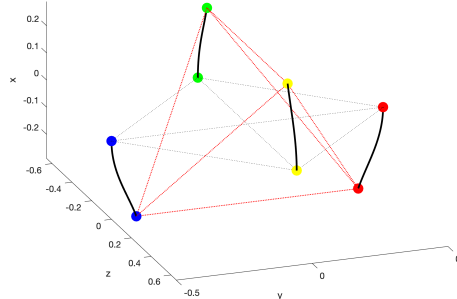


Figure 1: Non-trivial branch of balanced configurations bifurcating from the square configuration with four equal masses. As  $s$  decreases from  $\bar{s} = 1.4$ , the square deforms into a tetrahedron, which becomes regular at  $s = 1$ . All configurations along this branch are minima of  $U|_{\mathcal{S}}$ .

A second example starts with three unit masses at the vertices of an equilateral triangle and another unit mass at the barycenter. The non-trivial branch originates at  $\bar{s} = 2.5$  (see Figure 2). In this case, all configurations along the branch are saddle points of  $U|_{\mathcal{S}}$ . By varying the mass at the center while keeping the other three equal to 1, we observe a critical value

$$m^* = \frac{2 + 3\sqrt{3}}{18 - 5\sqrt{3}},$$

at which the initial planar configuration becomes degenerate. For  $m_4 < m^*$ , the solutions are minima of  $U|_{\mathcal{S}}$ . As  $m_4$  increases and approaches  $m^*$ , the solutions transition from minima to saddle points, and then back to minima near  $s = 1$ . At these transitions, the system's stability changes, and new branches of solutions should arise, though we were unable to identify them numerically. For  $m_4 > m^*$ , the solutions begin as saddle points and later become minima.

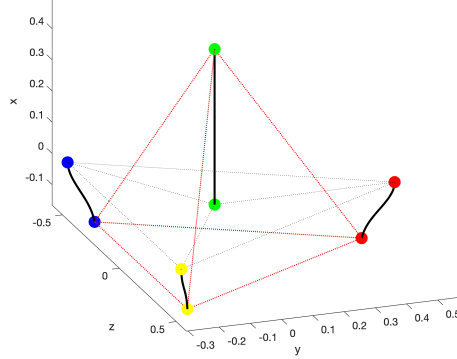


Figure 2: Non-trivial branch bifurcating from the triangular configuration with a central mass. The branch originates at  $\bar{s} = 2.5$ . For equal masses, all solutions along the branch are saddles. Varying the central mass reveals a critical value  $m^*$  at which the stability type changes.

## 6.2 Examples for $n = 5$

We now place four unit masses at the vertices of a square and one unit mass at the barycenter. In this case, there are two bifurcation points:  $s_1 = 2.5$  and  $s_2 = 1.2$ . From the first bifurcation point, a branch emerges along which the parameter  $s$  decreases. At  $s = 1$ , the masses form the vertices of a regular square pyramid (see Figure 3). These configurations are local minima of  $U|_{\mathcal{S}}$ . From the second bifurcation point, as  $s$  decreases, the configuration at  $s = 1$  becomes a tetrahedron with  $m_5$  at the barycenter (see Figure 4). These are saddle points of  $U|_{\mathcal{S}}$ . Furthermore, there exists a critical value  $m^*$  of  $m_5$  above which the nature of the configurations changes. For  $m_5 < m^*$ , the configurations along the first non-trivial branch are initially local minima but eventually transition into saddle points. For  $m_5 > m^*$ , these configurations are always saddle points. The second branch is unaffected by this change.

## 7 Numerical simulations for collinear balanced configurations

We conclude by presenting numerical examples of bifurcations in collinear central configurations for the four-body problem. In [4], numerical simulations were carried out for the three-body case; here, we extend that work to four bodies. Recall that for this problem we work in  $\mathbb{R}^2$  with

$$S = \text{diag}(s, 1).$$

Collinear central configurations on  $\{0\} \times \mathbb{R}$  are solutions of the balanced configuration equation for all  $s > 1$ , forming a trivial branch of solutions. For each choice of mass ordering along the  $y$ -axis, there are at least  $n - 2$  bifurcation instants. In particular, for  $n = 4$  there are always at least two.

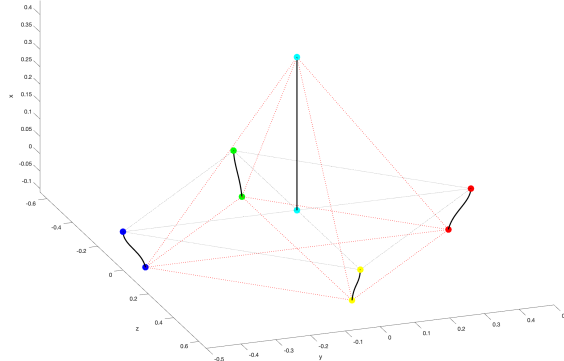


Figure 3: Non-trivial branch for five equal masses originating at  $s_1 = 2.5$ . As  $s$  decreases, the configuration evolves from a square with a central mass into a regular square pyramid at  $s = 1$ . These solutions are minima of  $U|_{\mathcal{S}}$ .

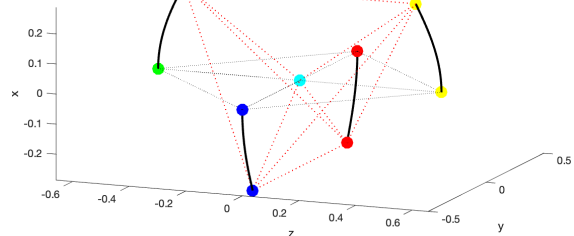


Figure 4: Non-trivial branch for five equal masses originating at  $s_2 = 1.2$ . As  $s$  decreases, the configuration becomes a tetrahedron with the fifth mass at the barycenter. These solutions are saddles of  $U|_{\mathcal{S}}$ .

In the first example, see Figure 5, we assume that all masses are equal to 1. There are two bifurcation instants,  $s_1 = 4.15$  and  $s_2 = 2.4$ . Along the non-trivial branch originating from the first bifurcation, the parameter  $s$  initially decreases until it reaches a turning point, where the masses form the vertices of a rhombus. Beyond this point,  $s$  increases again until reaching another turning point, where the masses realign along the line, but with the two central masses swapped.

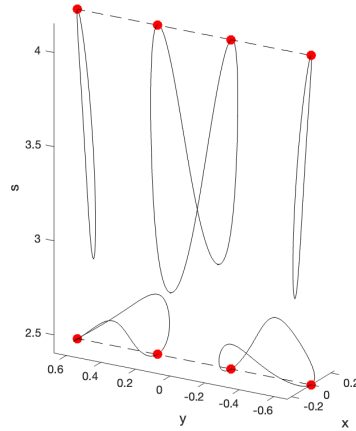


Figure 5: Non-trivial branches for four equal masses. The branch from  $s_1 = 4.15$  passes through a rhombus configuration before returning to a collinear alignment, with the two central masses exchanged; all solutions are minima. The branch from  $s_2 = 2.4$  also returns to a collinear alignment but with both pairs swapped; all solutions are saddles.

In the plane  $x\hat{O}y$ , the two central masses appear to rotate around a common point, while the external masses oscillate. All these solutions are local minima of  $U|_{\mathcal{S}}$ . Since the stability does not change after the turning point, we expect additional branches to bifurcate from this turning point, though we were unable to identify them numerically. Along the second non-trivial branch,

the parameter  $s$  first increases, reaches a turning point, and then starts decreasing until another turning point is reached. At this point, the masses realign along the line, but with the first and second masses swapped, as well as the third and fourth masses. These solutions are all saddle points of  $U|_{\mathcal{S}}$ .

We now present some examples where the last two masses are set to 1 (represented by the red dots in the figures), while the first two masses are equal to  $\alpha < 1$  (represented by the blue dots). For  $\alpha = 0.2$ , we observe two bifurcation points,  $s_1 = 4.9$  and  $s_2 = 1.9$ . Along the non-trivial branch originating from the first bifurcation point, we identify two turning points. The smaller masses continue to rotate around a common center, while the unitary masses oscillate (see Figure 6). At the first turning point, a new non-trivial branch detaches, along which the parameter  $s$  decreases until it reaches another turning point, and then approaches a limit configuration as  $s \rightarrow +\infty$ . The solutions along the original non-trivial branch are minima, while those on the branch originating from the turning point are saddles. For homological reasons, we also expect another branch to detach from the turning point, along which the parameter  $s$  increases. Along the branch originating from the second bifurcation point, the parameter  $s$  decreases until a turning point is reached, and then approaches a limit configuration as  $s \rightarrow +\infty$  (see Figure 7). All the solutions along this branch are saddle points.

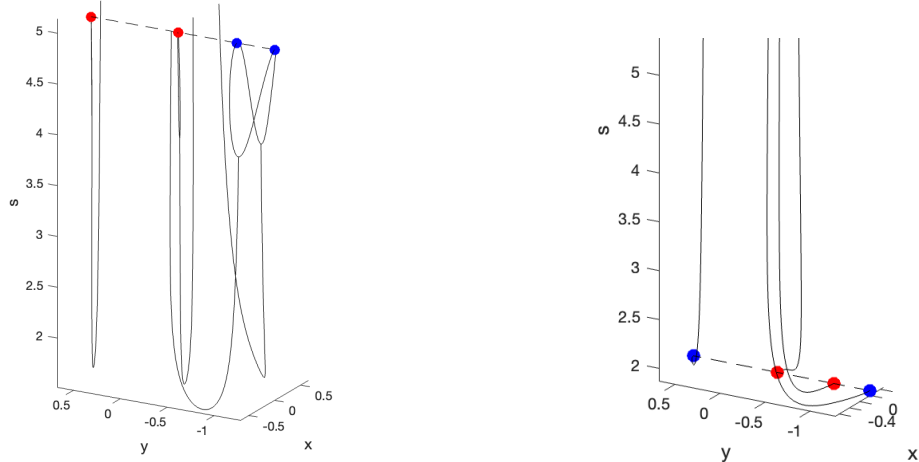


Figure 6: Non-trivial branch for masses  $[0.2, 0.2, 1, 1]$  originating at  $s_1 = 4.9$ . The smaller masses rotate around each other while the bigger masses oscillate. At the first turning point, a new branch detaches, containing only saddles.

Figure 7: Non-trivial branch for masses  $[0.2, 0.2, 1, 1]$  originating at  $s_2 = 1.9$ . Along this branch the parameter  $s$  decreases, and the configuration tends toward a limit as  $s \rightarrow +\infty$ . All solutions are saddles.

For  $\alpha = 0.5$ , see Figure 8, we observe two bifurcation instants,  $s_1 = 4, 3$  and  $s_2 = 2, 2$ . Along the non-trivial branch originating from the first bifurcation point, the parameter  $s$  initially decreases until a turning point, after which it increases, while the configuration approaches a limit configuration for  $s \rightarrow +\infty$ . These configurations are initially minima of  $U|_{\mathcal{S}}$ , but as they reach the turning point, they become saddle points. The branch originating from the second bifurcation exhibits a intricate behaviour, with the masses of equal value oscillating around each other. All of these solutions are saddle points.

Finally, for  $\alpha = 0.9$  (Figure 9), we observe a behaviour similar to those encountered previously.

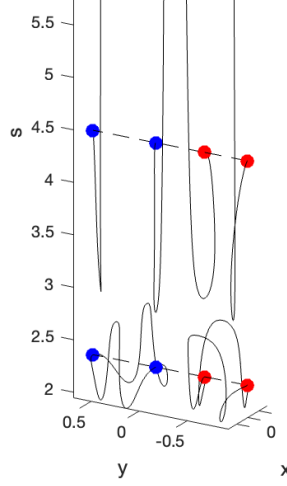


Figure 8: Non-trivial branches for masses  $[0.5, 0.5, 1, 1]$ . The branch from  $s_1 = 4.3$  first consists of minima, but after a turning point the solutions become saddles. The branch from  $s_2 = 2.2$  exhibits oscillations between equal masses and consists entirely of saddles.

The branch originating from the first bifurcation point follows a similar path to the branch originating from the first bifurcation point in the case of  $\alpha = 0.5$ . The branch originating from the second bifurcation point, on the other hand, resembles the one originating from the second bifurcation point in the equal masses case.

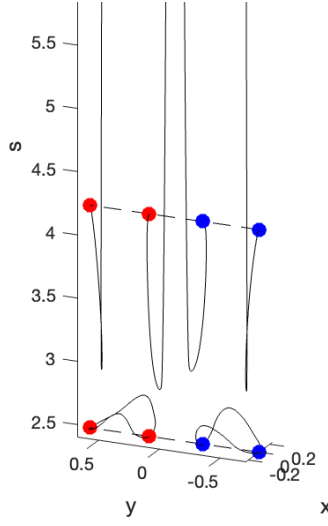


Figure 9: Non-trivial branches for masses  $[0.9, 0.9, 1, 1]$ . The branch from the first bifurcation behaves like the  $\alpha = 0.5$  case, with a stability change at a turning point. The branch from the second bifurcation resembles the equal-mass case, consisting entirely of saddles.

These are just a few of the possible collinear configurations for the four-body problem. We have selected them to highlight some of the most interesting behaviours.

**Remark 7.1.** We expect to find new branches originating from turning points, especially when the stability nature of the critical points does not change before and after the turning point, since the local homology remains unchanged. We attempted to perturb along a kernel direction near the turning point, as well as along random directions, but were not always successful in identifying these new branches. For the masses  $[0.2, 0.2, 1, 1]$ , we were able to find one branch detaching from a turning point, even though we expected another one based on homological considerations. A possible approach to improve our analysis could involve calculating the Conley index at the critical points, which might provide more precise information about the dynamics near these turning points and help confirm the existence of additional branches. Also various numerical approaches to switching branches at bifurcation are discussed in [9].

## References

- [1] Alain Albouy and Alain Chenciner. Le problème des  $n$  corps et les distances mutuelles. (french) [The  $n$ -body problem and mutual distances]. *Inventiones Mathematicae*, 131(1):151–184, 1998.
- [2] Eugene L. Allgower and Kurt Georg. *Numerical Continuation Methods*. Springer Series in Computational Mathematics. Springer Berlin Heidelberg, 1990.
- [3] Luca Asselle and Alessandro Portaluri. Morse theory for  $S$ -balanced configurations in the Newtonian  $n$ -body problem. *Journal of Dynamics and Differential Equations*, 35:907–946, 2021.
- [4] Luca Asselle, Alessandro Portaluri, and Marco Fenucci. Bifurcation of balanced configuration for the Newtonian  $n$ -body problem in  $\mathbb{R}^4$ . *Journal of Fixed Point Theory and Applications*, 24(22), 2022.
- [5] Michael F. Atiyah, Vijay K. Patodi, and Isadore M. Singer. Spectral asymmetry and Riemannian geometry. III. *Math. Proc. Cambridge Philos. Soc.*, 79:71–99, 1976.
- [6] Patrick M. Fitzpatrick, Jacobo Pejsachowicz, and Lazaro Recht. Spectral flow and bifurcation of critical points of strongly-indefinite functionals part I. General theory. *J. Funct. Anal.*, 162(1):52–95, 1999.
- [7] Xijun Hu and Alessandro Portaluri. Index theory for heteroclinic orbits of Hamiltonian systems. *Calc. Var. Partial Differential Equations*, 56(6), 2017.
- [8] Xijun Hu and Alessandro Portaluri. Bifurcation of heteroclinic orbits via an index theory. *Math. Z.*, 292(1–2):705–723, 2019.
- [9] H. B. Keller. Lectures on numerical methods in bifurcation problems, 1986.
- [10] Richard Moeckel. Celestial mechanics (especially central configurations). Handwritten lecture notes, Trieste, 1994. URL: <http://www.math.umn.edu/~rmoeckel/notes/Notes.html>.

- [11] Richard Moeckel. Lectures on central configurations. Lecture notes, Centre de Recerca Matemàtica, January 2014. URL: <http://www.math.umn.edu/~rmoeckel/notes/CentralConfigurations.pdf>.
- [12] Joel Robbin and Dietmar Salamon. The spectral flow and the Maslov index. *Bulletin of the London Mathematical Society*, 27(1):1–33, 1995.